FEDSM-ICNMM2010-' 0) $&

KINEMATICS OF A FREE PARTICLE MOVING BETWEEN TWO PARALLEL WALLS

Champmartin Stéphane
Ecole Arts et Métiers ParisTech/EMT
2 bd du Ronceray, BP 93525, 49035 Angers
cedex 1, France

Ambari Abdlehak
Ecole Arts et Métiers ParisTech/EMT
2 bd du Ronceray, BP 93525, 49035 Angers
cedex 1, France

Ben Richou Abderrahim
EMET/Faculté des Sciences et
Techniques, BP 523,
Beni Mellal, Morocco

ABSTRACT

The understanding of some physical phenomena involved in the transport of free particles such as fibers during injection processes is an important issue. To answer some of the questions arising in such problems, we study here numerically the quasi-steady kinematics of a free cylindrical solid particle moving in a Newtonian fluid confined between two parallel plane walls taking the hydrodynamic interactions into account. This is achieved by the use of the resistance matrix technique relating the kinematics of the particle to the forces and the torques exerted on the particle and to the dissipation induced by the motion of this particle. Our approach is confirmed by asymptotical developments and by a comparison with other authors in some cases. The solutions of three practical problems are given. In the first one, the sedimentation of the particle is studied. It is found that the maximum settling velocity of the free particle is obtained at a position off the symmetry plane. The cylinder is observed to rotate counter intuitively against the direction of rolling along the adjacent wall. Moreover the angular velocity has an influence on the settling velocity when the concentration is very high. The second problem concerns the transport of a neutrally buoyant cylindrical particle in a Poiseuille flow. This study reveals that there are relative translational and angular velocities between the free particle and the undisturbed fluid particle contrary to the commonly admitted hypothesis used in several models and numerical codes. Finally the third problem is a combination of the two previous situations: the transport of a non-neutrally buoyant particle in a Poiseuille flow. Depending on the ratio of the buoyancy forces to the viscous ones, different solutions are possible and exposed. Other problems can also be solved with this approach which is less time-consuming than complex methods such as DNS.

INTRODUCTION

Situations in which transported particles are encountered are numerous [1]. Let us cite for instance the case of sedimentary particles; in the industry field, this phenomenon plays a role in oil engineering, filtration, in pharmaceutical and food industries, in the design of composite materials or in biomedical engineering. A correct understanding of the physical phenomena involved in such situations is therefore essential. The study of the flows past small particles goes back to the early works of Stokes [2] for the flow around a solid spherical particle. In infinite medium and for a finite cylinder of radius a and length l, when $l/a \gg 1$, Batchelor [3] developed the slender body theory based on the creeping flow equations. As discussed in a previous article [4], we showed that in a bounded medium (high concentration), the slender body approach and the Stokes type solution obtained for a cylinder in the creeping flow are similar.

The motions of particles in concentrated regimes are complicated because the hydrodynamic interactions slowly decay with distance and the kinematics of each particle depends on the motions of the nearby particles and is strongly affected in the near-wall regions. This is for example the case in the injection molding of fiber-reinforced thermoplastics where the

rheological properties of the material are very sensitive to the fiber orientation which affects the velocity profile of the flow. This sort of process is therefore characterized by a complex and strong coupling and it seems essential to control or at least to predict the orientation of the fibers during the injection phase. From a theoretical point of view, Jeffery [5] proposed in 1922 a first model for the evolution of the orientation of a solid ellipsoidal particle in infinite medium. When many particles interact (concentrated regime), it is not possible anymore to assume that each particle moves at the same velocity as the fluid. Notice that many proposed models to describe the evolution of transported particles such as Folgar et al's [6] do not properly take the hydrodynamic interactions into account.

To overcome the theoretical difficulties due to these interactions, various numerical methods are available. They belong to three main families: the first one is the two-fluid model which treats each phase as a separate fluid with its own set of governing balance equations. Each phase has its own velocity, temperature and pressure. The main difficulty in this type of approach is to correctly calculate the interaction term between both phases. The second family of numerical methods, called LNS methods (Lagrangian Numerical Simulation), consists in tracking each particle when the evolution of the hydrodynamic fields is known, this latter being often computed with an Eulerian method. The main problem in these methods is the correct estimation of the hydrodynamic interactions between the particles. The third approach is known as the DNS methods (Direct Numerical Simulation). They consist in solving exactly the Stokes equations for the fluid phase and the Newton equations for the solid phase taking the whole interactions into account. The particles are not defined as points associated with forces and torques but by their own intrinsic characteristics such as their shape or volume. This kind of methods is often used to solve problems dealing with sedimenting particles (see for instance the work of Hu et al. [7] or of Pan et al. [8]). Unfortunately, they are very time-demanding and as such they often require the use of massive computer ressources.

As mentioned above, both the analytical and numerical methods available to solve two-phase flow problems are very complex. In the present work, we chose a completely different approach, based on the generalized resistance matrix technique, in order to obtain the quasi-steady kinematics of a free cylindrical particle in three classical situations: the first one is the sedimentation of a particle, the second is the transport of a neutrally buoyant particle in a plane Poiseuille flow and the third is the transport of a non-neutrally-buoyant particle in the same plane Poiseuille flow. Notice that this quasi-steady approach does not account for inertial effects such as lateral migration (Segré-Silberberg effect [9]). In the next paragraph, the method and the studied system are described.

DESCRIPTIONS OF THE METHOD AND THE MODEL

The main goal is to determine the quasi-steady kinematics of a free particle and to assess the effects of the confinement (hydrodynamic interactions) and of the asymmetrical position on the particle. We will solve problems of a particle in stationary motion subject to hydrodynamic interactions from two parallel walls at very low Reynolds numbers. In order to evaluate these effects, we intentionally limit the complexity of the system and we study an infinitely long cylindrical particle moving through a Newtonian fluid as justified in [4]. This latter assumption allows separating the effects due to the hydrodynamic interactions (confinement and asymmetry) from the effects due to the complex behavior of the fluid. We also suppose that the particle moves parallel to the walls and that the axis of the particle remains perpendicular to the direction of motion.
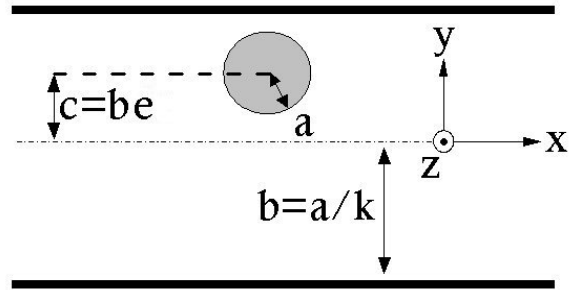

Fig. 1 - Sketch of the problem

The geometry of the problem is presented in Fig. 1. The radius of the particle is called a, half the distance between the parallel walls is called b and the distance between the axis of the particle and the symmetry plane is called c. The dimensionless groups $k = a/b$ and $e = c/b$ are respectively called the confinement and the eccentricity parameters. The problem of the two-dimensional flow around a circular particle moving in an unlimited medium when the inertial effects are neglected is characterized by the existence of the well-known Stokes paradox highlighted by Oseen [10] in 1910 and solved by Lamb [11] shortly afterwards: for such a problem, there is no solution to the Stokes equations that obeys both the boundary conditions at infinity and at the particle wall. However in confined situations, it was demonstrated that Stokes type solutions exist for such a cylindrical particle. Then the solution of the Navier-Stokes equations at very low Reynolds numbers leads to the existence of a proportionality relationship between the force and the velocity (Stokes type solution). In fact this result is much more general and it is possible to show that a particle moving at the velocity $\vec{U} = U_x \vec{e}_x + U_y \vec{e}_y$ and rotating at the angular velocity $\vec{\Omega} = \Omega_z \vec{e}_z$ undergoes some forces and torques proportional to these velocities. Therefore at very low Reynolds number, we can introduce to the first order of the inertia effetcs a matrix, called the resistance matrix, linking the kinematics of the particle to the forces and torques exerted on it:

$$\begin{bmatrix} F_x \\ F_y \\ M_z/a \\ \Delta P2b \end{bmatrix} = \mu\left(\overline{\overline{M}}_0 + \mathrm{Re}\,\overline{\overline{M}}_{iner}\right) \begin{bmatrix} U_x \\ U_y \\ \Omega_z a \\ \overline{U} \end{bmatrix} \qquad (1)$$

where

$$\overline{\overline{M}}_0 = \begin{bmatrix} A_{11} & 0 & A_{13} & A_{14} \\ 0 & A_{22} & 0 & 0 \\ A_{31} & 0 & A_{33} & A_{34} \\ A_{41} & 0 & A_{43} & A_{44} \end{bmatrix} \qquad (2)$$

represents the Stokes type, non-inertial part of the solution of the Navier-Stokes and continuity equations:

$$\begin{cases} \vec{\nabla}.\vec{u} = 0 \\ \rho\left[\dfrac{\partial \vec{u}}{\partial t} + (\vec{u}.\vec{\nabla})\vec{u}\right] = -\vec{\nabla}P + \mu\nabla^2\vec{u} \end{cases} \qquad (3)$$

with adapted boundary conditions to each configuration. Notice that all the terms due to inertia in the matrix $\overline{\overline{M}}_0$ are taken to be zero and that this matrix is symmetrical (Happel et al [12]). The inertial part of the solution of (3) is thus transferred into the matrix $\mathrm{Re}\,\overline{\overline{M}}_{iner}$. The determination of the coefficients A_{ij} is achieved with four series of numerical simulations: in the first one, the particle translates without any angular velocity, at the velocity U_x along the parallel walls through a quiescent fluid. This first series fills the first column of the resistance matrix. The second one is similar but the motion is in a direction perpendicular to the walls at velocity U_y. The third series of simulations concerns the flow generated by the rotation of the particle around its axis at angular velocity Ω_z in an otherwise fluid at rest. The fourth column is finally completed with the simulation of a fixed particle in a plane Poiseuille flow of mean velocity $\overline{U}$.

The numerical calculations were done using the finite volume technique and a projection method. The set of equations (3) is solved adimensionally with a two-step fractional-step procedure based on an article of Ye et al [13] and discretized using a fully orthogonal rectilinear grid. A second order Adams-Bashforth scheme was employed for the convection terms and the diffusion terms with an implicit Crank-Nicholson scheme. The numerical resolution of the various systems of algebraic equations was performed using the well-known SOR iterative method. A validation was done with asymptotic developments and finally the results are compared to those obtained with the commercial CFD code Fluent. Both comparisons successfully confirm the accuracy of our code. In order to avoid the numerical difficulties related to the motion of the particle when it moves parallel to walls, we solved the equivalent problem of a fixed particle with parallel walls moving at the same velocity. However this artifice cannot be

used anymore for the perpendicular motion to compute A_{22} and so we used the fact that for very low velocity and very large kinematic viscosity ($\mathrm{Re} \ll 1$), the quasi-steady state is established, inducing a negligible error in the position of the particle and the transient regime is reduced due to the weakness of the vorticity diffusion time scale $\tau = a^2/\nu$. The results obtained by this method were successfully compared to those obtained using a dynamic mesh technique implemented in the commercial CFD package Fluent.

RESULTS AND DISCUSSION
In this paragraph, we successively present the results concerning the problems of the sedimentation of a solid particle, of a neutrally buoyant particle in a Poiseuille flow and of a non-neutrally buoyant particle in the same Poiseuille flow. We only report here the data concerning the translational and angular velocities but the results concerning the additional pressure losses were also determined in the same manner.

Case N°1: sedimentation of a particle
Let us study the sedimentation of a particle in a direction parallel to the vertical plane walls when gravity is directed in the positive x direction. If the difference between the particle density and the fluid density is called $\Delta\rho$ and when the steady-state sedimentation is reached, we can write:

$$\begin{cases} F_x = -\Delta\rho g \pi a^2 \\ M_z = \overline{U} = 0 \end{cases} \qquad (4)$$

The apparent weight of the particle balances the drag force, the torque on the particle and the mean flow are nil. With the conditions (4) and inverting the resistance matrix $\overline{\overline{M}}_0$, we obtain from (1) when $\mathrm{Re}\,\overline{\overline{M}}_{iner} = 0$:

$$U_x^S = \left(\frac{-A_{33}}{A_{11}A_{33} - A_{13}A_{31}}\right)U^* \quad (5)$$

$$\Omega_z^S = \left(\frac{A_{31}}{A_{11}A_{33} - A_{13}A_{31}}\right)\frac{U^*}{a} \quad (6)$$

with:

$$U^* = \frac{\Delta\rho g \pi a^2}{\mu} \qquad (7)$$

a characteristic velocity of the sedimentation. Let us recall that equations (5) and (6) are valid only in the limit of small particle Reynolds numbers. In our study, this is verified at least up to:

$$\mathrm{Re}_S = \frac{\rho U_x^S 2a}{\mu} = 0.01$$

with ρ the fluid density. However we know that the confinement delays the advent of the inertial effects and the limit given here may become higher if the confinement becomes more important. In the article of Feng et al [14], the lateral drift of the settling particle due to inertia is obtained for a particle Reynolds number 10 times greater than here.

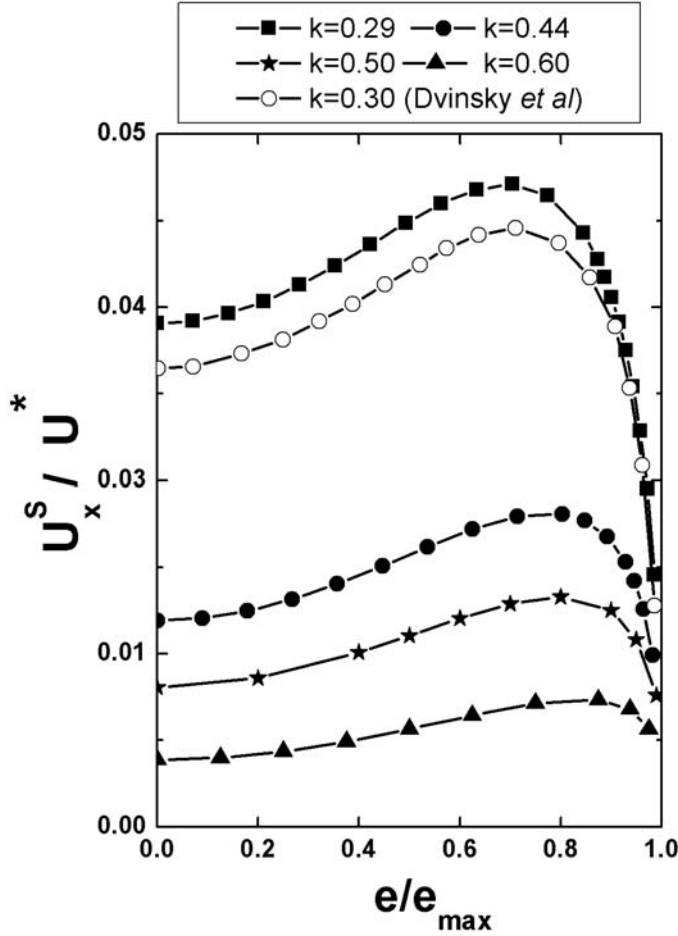Therefore in the present study, it is acceptable to neglect the lateral migration of the particle.

Fig. 2 - Sedimentation velocity vs transversal position

In Fig. 2, we report the evolution of the sedimentation velocity according to the eccentricity parameter e/e_{max} for four confinement parameters ranging between $k = 0.29$ and $k = 0.6$. Let us recall that the confinement parameter $k = a/b$ varies between 0 when the particle moves in an unbounded medium and 1 when the particle fills the whole space between the parallel plane walls (total blockage). The eccentricity parameter $e = c/b$ varies between 0 when the particle moves halfway between the parallel plane walls and $e_{max} = 1 - k$ when the particle touches one of the parallel walls. The main result clearly visible in Fig. 2 is the non-monotonous variation of the sedimentation velocity with the transversal position. The location of maximum sedimentation velocity is off the symmetry plane, at a position depending on the confinement parameter k. As the parameter k decreases, the position of maximum velocity gets closer to the symmetry plane $e/e_{max} = 0$. For instance for $k = 0.29$, the maximum velocity is reached at $e/e_{max} \approx 0.7$ whereas for $k = 0.44$, it is obtained

at $e/e_{max} \approx 0.8$. It must be also emphasized that the relative increase of the maximal sedimentation velocity with regard to the velocity in the symmetry plane grows when the confinement parameter increases. For $k = 0.29$, the maximal sedimentation velocity is about 28% greater than the velocity in the symmetry plane and for $k = 0.6$, the increase reaches almost 90% (for such a confinement, the particle moves nearly twice as fast as in the symmetry plane). We also compare our results for $k = 0.29$ with those obtained by Dvinsky et al [15] who numerically studied the same problem but for $k = 0.30$. In their study, they use a coordinate transformation of the governing equations expressed in the vorticity-stream function formulation based on the resolution of two elliptic partial differential equations. We can see that the trends are similar, with an optimum occurring at the same lateral position at $e/e_{max} \approx 0.7$. However, our data are higher than those of Dvinsky et al (maximum difference of 10% for $e/e_{max} = 0$) but this discrepancy can be attributed to the difference in the confinement parameters. The study of Fig. 2 could lead to the misunderstanding that a small particle would move faster than a large particle. We must keep in mind that the sedimentation velocity plotted in Fig. 2 is normalized with the characteristic velocity given by equation (7) in which the particle size a appears.

If we now rather consider the case of particles of various sizes falling in the same tank of constant dimension b, it is more relevant to plot the sedimentation velocity normalized with the new characteristic velocity:

$$U^{**} = \frac{\Delta \rho g \pi b^2}{\mu} = \frac{U^*}{k^2} \quad (8)$$

For the symmetrical position $e/e_{max} = 0$ for instance, the variation of U_x^S / U^{**} is plotted in Fig. 3 as a function of the confinement parameter k. In this particular plot, for a fixed wall separation b, the velocity of a particle falling in the symmetry plane reaches a maximum for a cylinder of critical radius $a_{cr} = 0.35b$. This non-intuitive result can be explained as follows: for particles such that $0 < a < a_{cr}$, the sedimentation velocity increases when the size of the particle increases. In this range the apparent weight of the particle, proportional to the square of the particle radius, grows faster that the drag force, resulting in an increase of the sedimentation velocity. On the other side for $a_{cr} < a < b$, the opposite situation occurs: when the radius grows, the increase of the drag force due to the backflow prevails over the increase of the apparent weight of the particle, leading to a decrease of the sedimentation velocity.
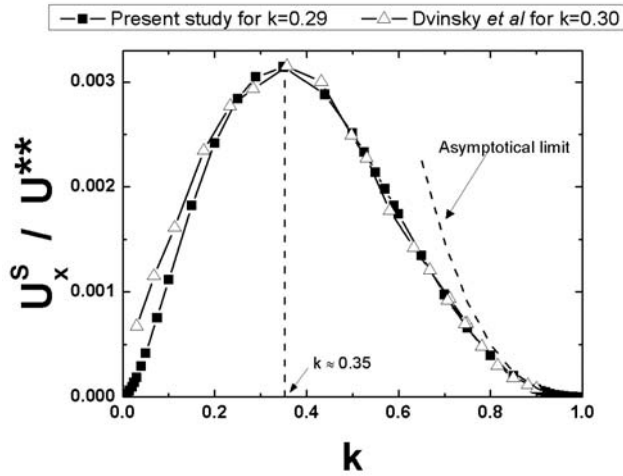
Fig. 3- Sedimentation velocity vs k for $e / e_{max} = 0$

We did an asymptotical development [4] in the lubrication regime for $k \to 1$. In this limit, the velocity behaves like the following equation:

$$\lim_{k \to 1} \frac{U_x^S}{U^{**}} \approx \frac{1}{9\pi} \sqrt{\frac{(1-k)^5}{2k}} \quad (9)$$

This relation is also plotted in Fig. 3 and accurately matches the numerical data in the lubrication regime. For $k = 0.9$ the relative difference between the asymptotical development and the numerical data is about 10% and it decreases to less than 1% for $k = 0.99$. Finally, the numerical results of Dvinsky *et al* [15] are also reported in figure 3 and satisfactorily agree with ours. A slight difference is obtained for the lowest confinement parameters. We showed in a previous study (see Fig. 4 in [4]) that the results of Dvinsky *et al*, when compared to various numerical, experimental and analytical studies, underestimate the drag force for $k < 0.25$ and thus inversely overestimate the settling velocity in this range.

In figure 4, we present the evolution of the angular velocity Ω_z^S given by equation (6) as a function of the transversal position in the channel. The main feature is the "anomalous" direction of rotation. If the particle settles along the positive x-axis in the region $y > 0$ as shown in Fig.1, it rotates clockwise and opposite to the direction of rolling on the upper wall. The opposite rotation direction is found if the particle is in the region $y < 0$. At the center of the channel, the particle does not rotate for obvious symmetry reasons. This phenomenon was already reported (see for instance [16], [17] and [18]) and is due to the blockage effect in the smallest gap when the particle is off the symmetry plane. Most of the backflow created by the particle motion goes between the particle and the furthest wall. This backflow imbalance creates the torque responsible for this "anomalous" rolling direction.
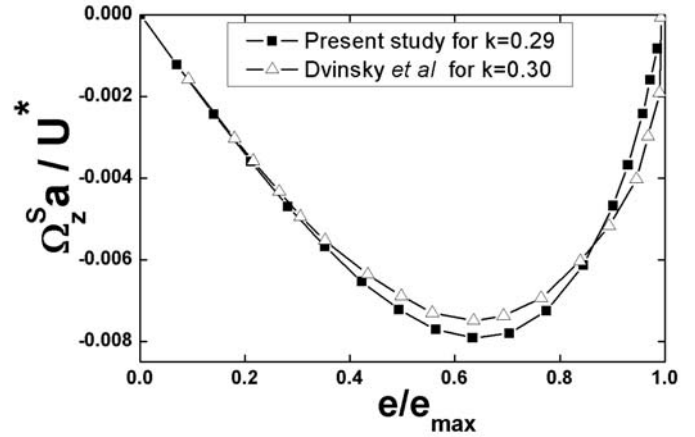

Fig. 4- Angular velocity vs transversal position

The comparison with the results of Dvinsky *et al* [15] presented in Fig. 4 is once again satisfactory, the difference in the confinement parameters accounting for slight discrepancy between both curves.

Finally, we investigated in Fig. 5 the influence of the angular velocity Ω_z^S on the settling velocity U_x^S of the particle for $k = 0.6$. When the rotation is impeded, we notice that the particle settles slower compared to the free particle configuration. When we looked at the pressure field around the free particle, it was observed that the rotation of the particle induces a lower pressure upstream and a higher pressure downstream. This pressure difference explains the enhanced settling velocity for the completely free particle.
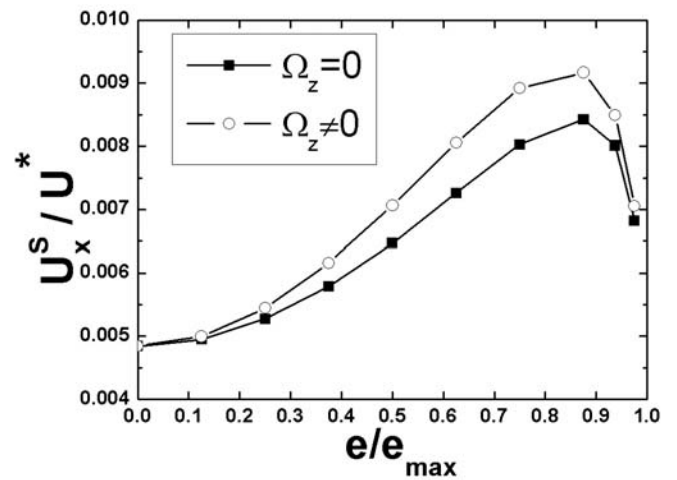

Fig. 5- Sedimentation velocity vs transversal position with or without angular velocity for $k = 0.6$

Case N°2: transport of a neutrally buoyant particle in a plane Poiseuille flow

Now we suppose that the fluid and the particle have the same density and that the particle is transported in a plane Poiseuille flow of mean velocity $\overline{U}$:

$$u(y) = \frac{3\overline{U}}{2}\left(1 - \frac{y^2}{b^2}\right) \quad (10)$$

If the particle is free to move and when the steady state is reached, the particle is in dynamic equilibrium and the sum of the external forces and torques acting on it is zero. Hence we can write:

$$\begin{cases} F_x = M_z = 0 \\ \overline{U} \neq 0 \end{cases} \quad (11)$$

The resolution of the system yields:

$$U_x^P = \left(\frac{A_{13}A_{34} - A_{14}A_{33}}{A_{11}A_{33} - A_{13}A_{31}}\right)\overline{U} \quad (12)$$

$$\Omega_z^P = \left(\frac{A_{31}A_{14} - A_{11}A_{34}}{A_{11}A_{33} - A_{13}A_{31}}\right)\frac{\overline{U}}{a} \quad (13)$$

Let us recall that equations (12) and (13) are valid only in the limit of small bulk and particle Reynolds numbers. In this study, this is verified at least up to:

$$\mathrm{Re}_{\overline{U}} = \frac{\rho \overline{U} 2b}{\mu} = 0.01$$

$$\mathrm{Re}_P = \frac{\rho U_x^P 2a}{\mu} = 0.01$$

In the article of Feng *et al* [17], the lateral migration, computed with a DNS simulation, is present for bulk and particle Reynolds numbers of 0.625 and 40 respectively. In the present study, the Reynolds numbers are much smaller and it is legitimate to neglect lift forces and lateral migration phenomena. In Fig. 6 we present the variation of the transport velocity of the particle according to the transversal position for various confinement parameters. We can see in this graph that the maximal transport velocity is always obtained in the symmetrical position for $e/e_{max} = 0$. Then this velocity continuously decreases as the particle gets closer to a wall. Another result is the existence of two regions: an inner region roughly for $e/e_{max} < 0.5$ in which the smaller the size of the particle, the faster the particle is transported and an outer region for $e/e_{max} > 0.5$ in which the opposite trend occurs. The most significant result is however obtained when we compare the transport velocity and the velocity of the undisturbed Poiseuille flow. This comparison is shown in Fig. 7 for the single confinement parameter $k = 0.29$. This graph reveals that the particle is always transported with a lesser velocity than the Poiseuille flow: there is a relative velocity for the transported particle. The further from the symmetry plane, the larger this relative velocity.
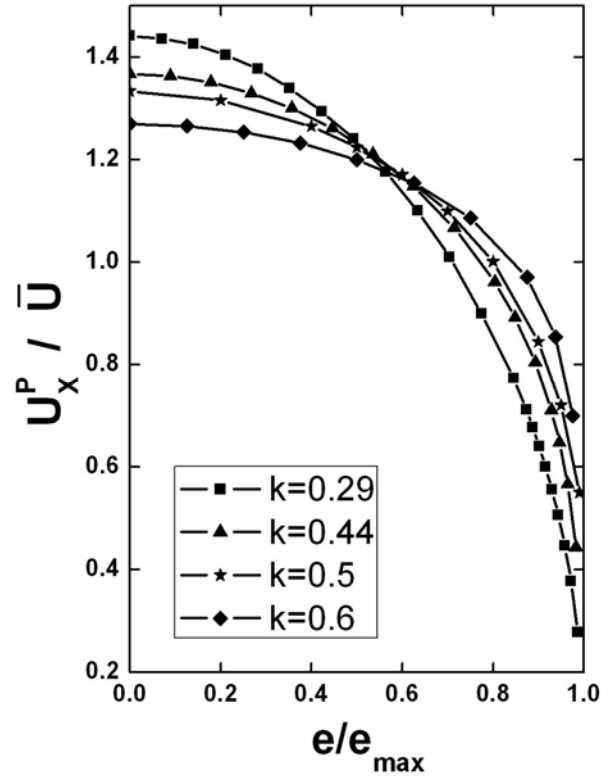

Fig. 6 - Transport velocity of a neutrally buoyant particle in a plane Poiseuille flow versus transversal position

These results unambiguously contravene the hypothesis of Jeffery [5] and used by Folgar *et al* [6] in their models to describe the behavior of particles in shear flows (they assume that a particle moves at the same velocity as the undisturbed flow).
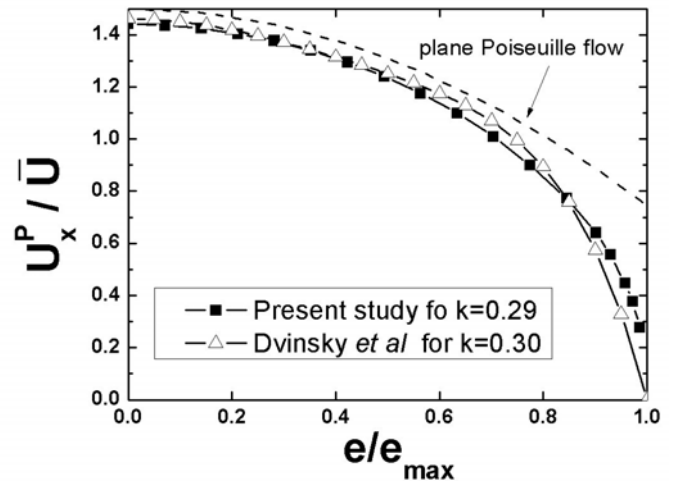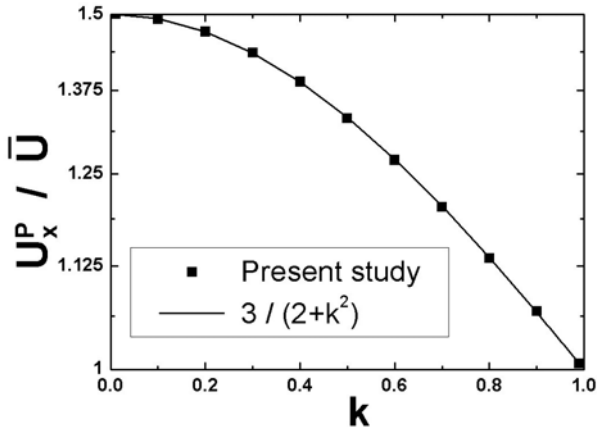

Fig. 7 - Transport velocity of a neutrally buoyant particle in a plane Poiseuille flow vs transversal position

This assumption should be reviewed in the cases of large hydrodynamic interactions, in particular in regions with high particle concentrations and/or in the near-wall regions. We also report in figure 7 the numerical results of Dvinsky et al [19] for the slightly different confinement parameter $k = 0.30$. The comparison is satisfactory except in the vicinity of the wall as $e/e_{max} \to 1$.

When the particle moves in the symmetrical position $e/e_{max} = 0$, we find that the effect of the confinement is given by a simple relationship such as:

$$\frac{U_x^P}{\overline{U}}(e/e_{max} = 0) = \frac{3}{2+k^2} \quad (14)$$

This expression is plotted in Fig. 8 together with the numerical data. The agreement between both approaches is very satisfactory. In the limit $k \to 0$, it is found that the particle moves with the velocity $3\overline{U}/2 = U_{max}$. Thus it is transported at the same velocity as the undisturbed flow.

Fig. 8 - Transport velocity of a neutrally buoyant particle in a plane Poiseuille flow versus k for $e/e_{max} = 0$

In the opposite limit $k \to 1$, it is observed that the particle moves with the mean velocity $\overline{U}$: the particle behaves like a plug and is pushed at the same speed as the mean flow. The maximum relative velocity obtained for $k \to 1$ is equal to 33% of the particle fluid velocity U_{max}.

Finally in Fig.9, we plot the evolution of the angular velocity according to the transversal position of the particle. Contrary to the sedimentation problem, the rotation direction of the particle is "normal". This is due to the velocity gradient in such a shear flow. The velocity of the Poiseuille profile is larger in the region close to the symmetry plane than near the walls. This induces a torque responsible for the observed rotation direction. In the same figure, we also reported the results obtained by Dvinsky et al [19] for $k = 0.30$ and both studies yield similar

results. Finally, we plotted the angular velocity of a fluid particle in the undisturbed Poiseuille flow:

$$|\vec{\omega}| = \frac{1}{2}|\vec{\nabla} \times \vec{u}|$$

The comparison reveals that although the angular velocities of the cylinder particle and of fluid particle are similar near the symmetry plane, they drift from each other as the cylindrical particle is close to a wall. Moreover, the angular velocity of the particle is always slower than the fluid particle and thus there exists too a relative angular velocity which should not be neglected for an accurate estimation of the particle transport characteristics.
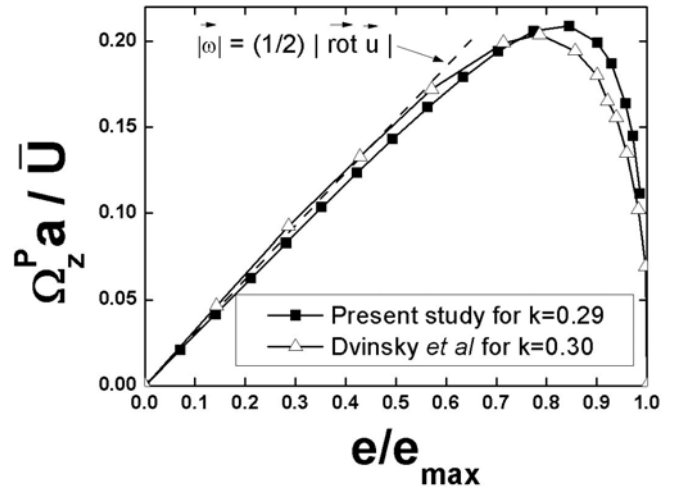
Fig. 9 - Angular velocity of a neutrally buoyant particle in a plane Poiseuille flow vs transversal position

Case N°3: transport of a non-neutrally buoyant particle in a plane Poiseuille flow

To evaluate a possible way to fractionate a polydispersed suspension, the last situation presented here is a combination of the two previous ones when the vertical Poiseuille flow is directed upwards and opposite to gravity. Because of the linearity of the system, the solution of a non-neutrally buoyant particle in a vertical plane Poiseuille flow is straightforwardly obtained by the superposition of the solutions of cases 1 and 2. Hence we find:

$$U_x^{P+S} = U_x^S - U_x^P = \left(\frac{-A_{33}}{A_{11}A_{33} - A_{13}A_{31}}\right)U^* \\ - \left(\frac{A_{13}A_{34} - A_{14}A_{33}}{A_{11}A_{33} - A_{13}A_{31}}\right)\overline{U} \quad (15)$$

In Fig. 10 we present the evolution of the transport velocity for a single confinement parameter $k = 0.29$ as a function of the transversal position. This velocity is scaled by the mean velocity of the Poiseuille flow $\overline{U}$. According to the above-written equation, we introduce a new parameter α such that:

$$\alpha = \frac{U^*}{\overline{U}} = \frac{\Delta\rho g \pi a^2}{\mu \overline{U}} \quad (16)$$

This dimensionless number compares the effects of the buoyancy force and the effects of the Poiseuille flow.
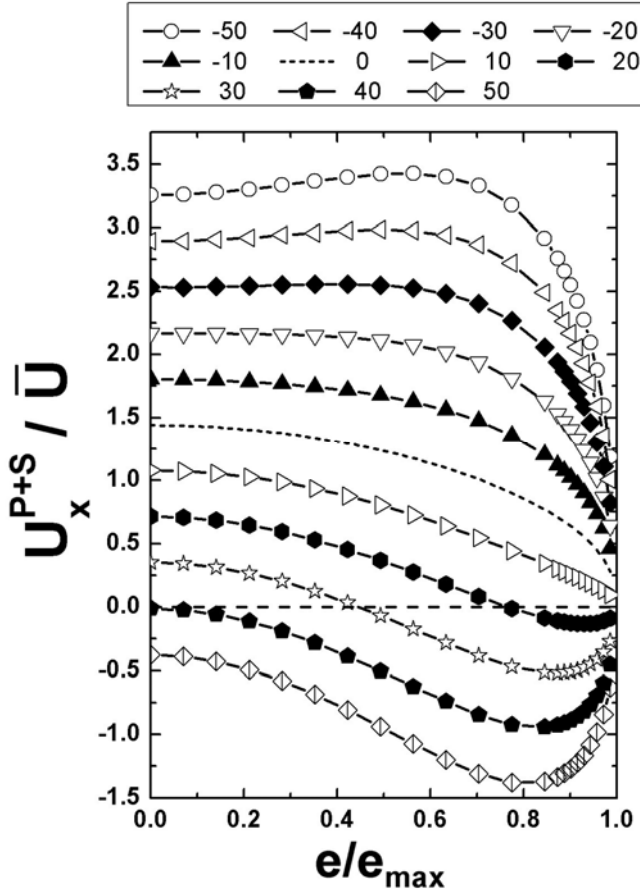
Fig. 10 - Transport velocity of a non-neutrally buoyant particle in a plane Poiseuille flow vs e/e_{max} for $k = 0.29$ and for various values of α

To the factor π, this number is also the ratio of the Archimedes and Reynolds numbers Ar and Re :

$$\alpha \propto \frac{\Delta\rho g a^3 \rho / \mu^2}{\rho \overline{U} a / \mu} = \frac{Ar}{Re} \quad (17)$$

The case $\alpha = 0$ corresponds to the neutrally buoyant particle studied in the previous section. The dotted curve for this case in Fig. 10 is exactly the same curve as in Fig. 7. When $\alpha > 0$, the particle is heavier than the carrying fluid so that the transport velocity is reduced by the effect of its sedimentation compared to the neutrally buoyant condition. Noteworthy is that it is possible to find situations for which the particle velocity is positive in an inner region and negative in an outer region. This

is clearly visible in Fig. 10 for $\alpha = 30$ for example. In this case, as long as $0 < e/e_{max} < 0.44$, the transport velocity is positive and the particle moves in the same direction as the Poiseuille flow (but with a large relative velocity). Globally the Poiseuille flow dominates sedimentation. For $0.44 < e/e_{max} < 1$ however, the velocity becomes negative and the Poiseuille flow cannot carry the particle anymore so that it settles in the direction opposite to the Poiseuille flow. In the near-wall region, the transport velocity induced by the Poiseuille flow become very low as can be seen in Fig. 7. This phenomenon could be used in particle or colloid analysis methods as an alternative to techniques such as Split-Flow Thin Fractionation (SPLITT cells). Indeed because α depends on the particle size a, the fractionation of a polydispersed sample could be performed. When α becomes greater than 40, the particle settles at any transversal position. Now when $\alpha < 0$, the particle is lighter than the fluid so that the opposite behavior occurs. The transport velocity is enhanced by the buoyancy whatever the transversal position of the particle.

CONCLUSION

In this work, we used the resistance matrix, the coefficients of which were numerically determined, in order to solve three practical problems involving a cylindrical particle in hydrodynamic interactions between two parallel walls. In this approach, we do not take into account inertial effects which induce any lateral migration because of the low values of the Reynolds numbers chosen here. Concerning the case of the sedimentation of the particle in a quiescent fluid, we showed the existence of a maximal settling velocity off the symmetry plane and of an "anomalous" rotation direction due to the backflow. When the particle settles symmetrically in a tank of fixed dimensions, we highlighted the non-intuitive existence of a critical particle radius at which the settling velocity is maximal. For the problem of the neutrally buoyant particle in a Poiseuille flow, we proved the existence of a relative translational and angular velocity between the particle and the undisturbed flow. Finally, in the problem of the non-neutrally buoyant particle in a Poiseuille flow we obtained positions at which the particle could be transported in the same direction as the carrying fluid and positions at which the direction of particle and of the Poiseuille flow are opposite. This result could lead to a new fractionation technique when the gravity is parallel to the flow direction. The results presented here emphasize the importance of the hydrodynamic interactions in the analysis of two-phase flow problems such as fiber transport at high particle concentrations or in the presence of confining walls. Others problems can be obtained once the resistance matrix is completed.

REFERENCES

[1] Clift R., Grace J. and Weber M. E., Bubbles, 2009, Drops and Particles. Dover Publications Inc.

[2] Stokes G. G., 1966, On the effect of the internal friction of fluids on the motion of pendulums. Cambridge Philos. Trans. 9, 8-106, 1851. Reprinted in Mathematical and Physical Papers, 2nd ed., Vol. 3. New York: Johnson Reprint Corp.

[3] Batchelor G. K., 1970, Slender-body theory for particles of arbitrary cross-section in Stokes flow. J. Fluid Mech **44**, 419-440.

[4] Champmartin S. and Ambari A., 2007, Kinematics of a symmetrically confined cylindrical particle in a "Stokes-type" regime. Physics of Fluids **19**, 073303.

[5] Jeffery G. B., 1922, The motion of ellipsoidal particles in a viscous fluid. Proc. Roy. Soc. London, **102**: 161-179.

[6] Folgar F. and Tucker C. L., 1984, Orientation behavior of fibers in concentrated suspensions. J. of Reinforced Plastics and Composites **3**, 98-119.

[7] Hu H. H., Joseph D. D., and Crochet M. J., 1992, Direct simulations of flows of fluid particle motions. Theor. Comput. Fluid Dyn. **3**, 285-306.

[8] Pan T. W. and Glowinski R., 2002, Direct simulation of the motion of neutrally buoyant circular cylinders in plane Poiseuille flow. J. Comp. Phys. **181**, 260-279.

[9] Segré G. and Silberberg A., 1961, Radial particle displacements in Poiseuille flow of suspensions. Nature **189**, 209-210.

[10] Oseen C. W., 1910, Uber die Stokessesche Formel und über eine verwandte Aufgabe in der Hydrodynamik. J. Ark. Mat. Astron. Fys., **29-6**, 1-20.

[11] Lamb H., 1911, On the uniform motion of a sphere in a viscous fluid. Philos. Mag. **21**, 112-119.

[12] Happel J. and Brenner H., 1965, Low Reynolds Number Hydrodynamics. Prentice-Hall.

[13] Ye T., Mittal H. S., Udaykumar H. S. and Shyy W., 1999, An accurate Cartesian grid method for viscous incompressible flows with complex immersed boundaries. J. Compt. Phys. **156**, 209-240.

[14] Feng J., Hu H. H. and Joseph D. D., 1994, Direct simulation of initial value problems for the motion of solid bodies in a Newtonian fluid. Part 1 Sedimentation, J. Fluid Mech. **261**, 95-134.

[15] Dvinsky A. S. and Popel A. S., 1987, Motion of a rigid cylinder between parallel plates in Stokes flow. Part 1: motion in a quiescent fluid and sedimentation. Comp. and Fluids, **15(4)**, 391-404.

[16] Liu Y. J., Feng J. and Joseph D. D., 1993, Anomalous rolling of spheres down an inclined plane. J. Non-Newtonian Fluid Mech. **50**, 305-329.

[17] Hu H. H., 1995, Motion of a circular cylinder in a viscous liquid between parallel plates. Theor. Comp. Fluid Dyn. **7**, 441-455.

[18] Feng J., Hu H. H. and Joseph D. D., 1994, Direct simulation of initial value problems for the motion of solid bodies in a Newtonian fluid. Part 2 Couette and Poiseuille flows, J. Fluid Mech. **277**, 271-301.

[19] Dvinsky A. S. and Popel A. S., 1987, Motion of a rigid cylinder between parallel plates in Stokes flow. Part 2: Poiseuille and Couette flow. Comp. and Fluids, **15(4)**, 405-419.